

Enhancing Heavy Rain Nowcasting with Multimodal Data: Integrating Radar and Satellite Observations

Rama Kassoumeh ¹ David Rügamer ^{2,3} Henning Oppel ⁴

¹Bochum Institute of Technology ²LMU Munich ³Munich Center for Machine Learning ⁴Okeanos Smart Data Solutions GmbH
rama.kassoumeh@bo-i-t.de david.ruegamer@stat.uni-muenchen.de henning.oppel@okeanos.ai

Abstract—The increasing frequency of heavy rainfall events, which are a major cause of urban flooding, underscores the urgent need for accurate precipitation forecasting—particularly in urban areas where localized events often go undetected by ground-based sensors. In Germany, only 17.3% of hourly heavy rain events between 2001 and 2018 were recorded by rain gauges, highlighting the limitations of traditional monitoring systems. Radar data are another source that effectively tracks ongoing precipitation; however, forecasting the development of heavy rain using radar alone remains challenging due to the brief and unpredictable nature of such events. Our focus is on evaluating the effectiveness of fusing satellite and radar data for nowcasting. We develop a multimodal nowcasting model that combines both radar and satellite imagery for predicting precipitation at lead times of 5, 15, and 30 minutes. We demonstrate that this multimodal strategy significantly outperforms radar-only approaches. Experimental results show that integrating satellite data improves prediction accuracy, particularly for intense precipitation. The proposed model increases the Critical Success Index (CSI) for heavy rain by 4% and for violent rain by 3% at a 5-minute lead time. Moreover, it maintains higher predictive skill at longer lead times, where radar-only performance declines. A qualitative analysis of the severe flooding event in the state of North Rhine-Westphalia, Germany on July 14, 2021 further illustrates the superior performance of the multimodal model. Unlike the radar-only model, which captures general precipitation patterns and light rainfall, the multimodal model yields more detailed and accurate forecasts for regions affected by heavy rain. This improved precision is critical for enabling timely, life-saving, and reliable early warnings during heavy rain events that have been repeatedly hitting Europe. The model implementation is available on GitHub ¹.

Index Terms—Nowcasting, Radar, Satellite, U-Net, Multimodal

I. INTRODUCTION

The prediction of heavy rainfall has become increasingly important in meteorological and hydrological research, especially in light of the rising frequency and intensity of such events due to climate change [1]. Accurate precipitation measurements are essential for real-time flood warning systems, yet current approaches often face limitations. Radar systems, while providing broader spatial coverage than ground-based sensors, measure precipitation indirectly at altitude. This in-

troduces significant uncertainty at ground level, often leading to the underestimation of localized heavy rain events [2].

Radar technology is a cornerstone of modern nowcasting systems due to its high spatial and temporal resolution—typically 1–2 km² every 5–10 minutes—and its ability to scan large areas [3]. This makes it well-suited for monitoring fast-evolving weather phenomena and issuing early warnings for convective events. Moreover, radar can detect atmospheric disturbances like thunderstorms before they produce measurable surface rainfall, providing valuable lead time for flood prevention [3]. However, radar also has limitations. It struggles to pinpoint the timing and location of initial raindrop formation, especially under complex summer conditions influenced by variables such as cloud height, instability, temperature, and humidity [4].

Even traditional ground-based rain gauges face critical limitations. Their measurements are restricted to a very small area—just a few meters around the sensor—and cannot capture the spatial heterogeneity of rainfall. For instance, in Germany, gauges detected only 17.3% of hourly heavy rainfall events between 2001 and 2018 [3]. This sparse coverage increases the risk of undetected extreme weather, particularly in urban regions with insufficient drainage infrastructure. The catastrophic floods in Germany in July 2021, which caused over 180 fatalities [2], and the floods in Austria in September 2024, where damages exceeded €1.3 billion and affected over 800 companies [5], emphasize the urgent need for more precise and timely heavy rainfall forecasting.

To better capture these fast-evolving weather conditions (especially during summer when heat and moisture trigger sudden downpours), meteorologists are increasingly turning to data fusion approaches. By combining radar and satellite data, forecasts can become more robust and spatially comprehensive.

Satellite imagery provides valuable complementary information by capturing a wide range of atmospheric and surface variables, such as land-water boundaries, snow and ice coverage, soil moisture, and vertical profiles of temperature and humidity [6]. Different spectral bands (visible, infrared, thermal, microwave) each contribute unique insights: infrared channels help estimate cloud-top temperatures and thickness,

¹https://github.com/RamaKassoumeh/Multimodal_heavy_rain

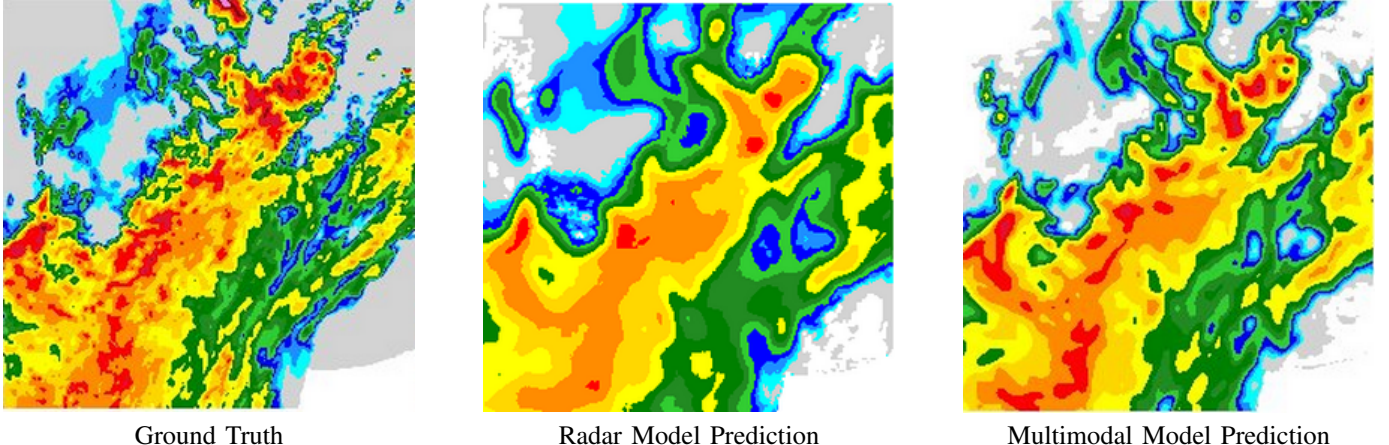


Fig. 1: The figure shows the ground truth of a flooding event in the state of North Rhine-Westphalia, Germany, on July 14, 2021, along with predictions from two models: Radar-only and Multimodal (Radar+Satellite) at a 30-minute lead time. Orange and red areas indicate heavy rainfall, with red representing higher precipitation intensities. This event led to catastrophic flooding in the region. The Multimodal model outperforms the Radar-only model, particularly in regions of intense rainfall where the Radar-only model fails to capture the full magnitude of the event. These results demonstrate that satellite data is crucial for accurate prediction of heavy rain scenarios. Capturing the correct magnitude of such events is essential for issuing timely warnings and enabling an effective first response, especially in light of similar extreme weather events that have recently occurred across Europe.

while microwave bands offer visibility into water vapor content and precipitation profiles. These capabilities make satellite data an essential component in both qualitative analysis and quantitative prediction of heavy rainfall events [6].

This paper focuses on processing satellite data from EU-METsat and radar data from national sources, and on developing models that combine both modalities. The main objective is to evaluate whether integrating satellite and radar data can improve the accuracy of short-term rainfall predictions. To ensure a fair comparison, we train two models based on a fixed architecture: one using only radar data, and another multimodal model using both radar and satellite data to assess the contribution of satellite information. The effectiveness of this multimodal approach is illustrated in Fig. 1, which compares predictions from both models during the catastrophic flooding event in North Rhine-Westphalia, Germany, on July 14, 2021.

II. RELATED WORK

This section reviews notable approaches for short-term precipitation nowcasting, with a focus on deep learning architectures designed to model spatiotemporal dynamics in weather data. The task is commonly framed as a spatiotemporal sequence forecasting problem, where the goal is to capture both temporal evolution and spatial context.

Recent research in precipitation nowcasting has explored various input–output modalities to improve forecast accuracy. Traditional models often perform radar-to-radar prediction, using sequences of past radar reflectivity frames to forecast future ones and capture local precipitation dynamics directly. Other approaches focus on satellite-to-satellite forecasting, predicting future satellite imagery based on prior observations

to model the temporal evolution of cloud and atmospheric features. Satellite-to-radar models have also emerged, aiming to infer radar reflectivity fields directly from satellite observations, enabling precipitation forecasts in areas with limited radar coverage. Multimodal models combining both satellite and radar inputs to predict future radar frames leverage the broad spatial coverage and spectral richness of satellites together with the direct precipitation measurements from radar, enhancing both spatial generalization and event-specific accuracy.

ConvLSTM [7] and RainNet [8] are radar-to-radar models that forecast future radar reflectivity maps from past observations. ConvLSTM extends traditional LSTMs by integrating convolutional operations into its gating mechanisms, enabling the joint modeling of spatial and temporal dependencies. RainNet, on the other hand, adopts a U-Net-like encoder–decoder architecture with skip connections to preserve spatial details and uses a log-cosh loss function to better capture extreme precipitation values. Both models are well-suited for spatiotemporal precipitation nowcasting and have influenced many follow-up works.

As a satellite-to-satellite forecasting model, DeePSat [9] predicts future satellite imagery using sequences of EUMET-SAT composites. It processes multi-channel inputs, including Day Microphysics, Severe Storm, and Water Vapor bands, to capture the temporal evolution of cloud and atmospheric structures. The model’s performance has been assessed using Mean Absolute Error (MAE) and Normalized MAE (NMAE), demonstrating its effectiveness in short-term satellite image prediction for nowcasting applications.

WeatherFusionNet [10] is a satellite-to-radar model that

predicts future radar frames using sequences of satellite images. While the architecture includes a module designed to take combined radar and satellite inputs, the final model uses only satellite data due to the poor quality of available radar observations. It leverages a Sat2Rad U-Net to extract precipitation-relevant features, followed by PhyDNet to model temporal dynamics, and a final U-Net to generate the radar-based forecast. A similar two-stage idea is explored in Sat2Rdr [11], where the model first predicts future satellite frames from past satellite sequences and then uses a separate satellite-to-radar model to convert the predicted satellite frames into precipitation radar images.

Our approach focuses on multimodal nowcasting, combining both satellite and radar inputs to predict future radar frames. Unlike methods that rely solely on satellite data, we utilize reliable radar observations to guide more accurate predictions. We conduct a comparative analysis of radar-only and radar-satellite models to assess the benefit of incorporating satellite imagery. While other studies often aim for year-round precipitation forecasting, our work specifically targets heavy rainfall during the summer period, as these events are among the most difficult to predict and are critical for the effectiveness of early warning systems.

III. METHODOLOGY

This section describes the data sources, the preprocessing, normalization procedures and evaluation metrics. It also presents the model architectures and loss functions employed in this study.

A. Data sources

This study focuses on the North Rhine-Westphalia (NRW) region in Germany during the summer months (May to August), when high temperatures increase evaporation and create favorable conditions for convective precipitation. Radar and satellite imagery from 2018 to 2021 were collected and pre-processed for the development and evaluation of nowcasting models.

Radar Data: High-resolution radar composites were provided by the German Meteorological Service (DWD) [12], which were generated by merging data from multiple radar stations and the quality was enhanced by hydro & meteo GmbH. The data include measurements from four radars: Neuheilenbach, Essen, Flechtdorf, and Hannover, with a spatial resolution of 1 km and a temporal resolution of 5 minutes. The dataset was cropped to cover roughly the NRW state, resulting in 288×288 pixel radar images, where each pixel corresponds to a precipitation value in mm/h, as shown in Fig. 2.

Following the classification defined by Barani Design Technologies [13], rainfall intensities are divided into light (0–2.5 mm/h), moderate (2.5–7.5 mm/h), heavy (7.5–50 mm/h), and violent (50–200 mm/h) categories. Pixels with missing or undefined values were labeled as -999 and treated as a separate category.

Satellite Data: Satellite data were acquired from the SEVIRI Level 1.5 rapid scan product by EUMETSAT, offering 11

spectral bands with 5-minute temporal resolution [14]. The original images, covering Europe and parts of the Middle East, were reprojected to EPSG:25832 (ETRS89 / UTM zone 32N) and cropped to the NRW state, yielding images of 47×92 pixels, as shown in Fig. 2.

The dataset includes spectral channels across the visible (VIS), near-infrared (NIR), infrared (IR), and water vapor (WV) ranges, supporting a wide range of meteorological observations. Note that VIS and NIR bands are only available during daytime.

Band Histogram Analysis: To explore potential correlations between satellite bands and rainfall intensity, histogram analyses were performed for light, moderate, heavy, and violent rain samples. For heavy rain events, two case studies on July 14, 2021 were analyzed using statistical tools including the Kolmogorov–Smirnov test and Kullback–Leibler divergence. The analysis revealed statistically significant differences between histograms of the two events across all bands, indicating that histogram-based features are not stable enough across samples for prediction. Consequently, raw satellite data were used as model input.

B. Data Preprocessing and Normalization

To ensure consistent and effective model training, several preprocessing and normalization steps were applied. First, radar images containing extreme outliers (>200 mm/h), accounting for 2.1% of the data, were removed due to reliability concerns. To address class imbalance, only 20% of no-rain images were retained. A 30-minute input window (6 consecutive images) was used, and sequences with missing radar or satellite files were discarded.

Radar values were normalized using a logarithmic transformation based on the precipitation maximum value (200):

$$x_{\text{norm}} = \begin{cases} \log_{202}(x + 2), & \text{if } x \geq 0 \\ 0, & \text{if } x = -999 \end{cases} \quad (1)$$

The base 202 accounts for the maximum value of 200, plus the shift (+2 total) to ensure numerical stability.

Satellite data, consisting of 11 bands, was normalized per band using Min-Max scaling:

$$X_{\text{norm}} = \frac{X - X_{\min}}{X_{\max} - X_{\min}} \quad (2)$$

where X_{\min} and X_{\max} were determined from the training set for each band separately.

C. Evaluation Metrics

To evaluate and compare the performance of the proposed models, two commonly used metrics in meteorological forecasting are employed: the Critical Success Index (CSI) and the Fractions Skill Score (FSS). These metrics capture different aspects of prediction quality and are well-suited to the specific challenges of precipitation nowcasting. The models are regression-based, outputting continuous rainfall estimates (mm/h). For evaluation purposes, these numerical outputs are

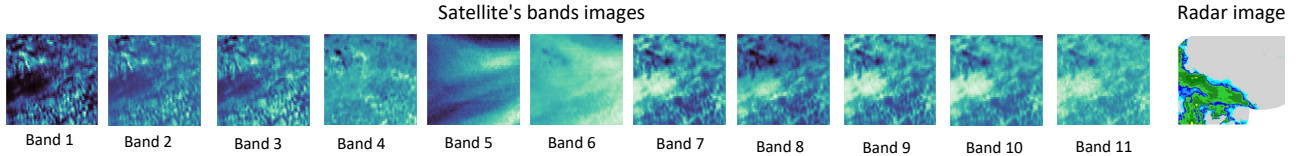


Fig. 2: Visualization of the 11 satellite bands and the radar image.

discretized into precipitation intensity categories, on which the metrics are then computed.

Critical Success Index (CSI): The Critical Success Index (CSI), also known as the Threat Score, is a categorical metric widely used in weather prediction. It assesses the ability of the model to correctly forecast the occurrence of precipitation exceeding a predefined threshold. It is particularly relevant when precise rainfall magnitudes are less critical than the correct detection of heavy rain events.

The CSI is computed based on a binary classification framework using a contingency table:

$$\text{CSI} = \frac{\text{TP}}{\text{TP} + \text{FP} + \text{FN}} \quad (3)$$

Where TP (True Positives) refers to cases where the model correctly predicted the rain category (e.g., heavy or violent rain), FP (False Positives) indicates cases where the model predicted a rain category that did not actually occur, and FN (False Negatives) denotes cases where a rain category occurred but was not predicted by the model. The CSI ranges from 0 to 1, where 0 indicates no skill and 1 represents a perfect score.

Fractions Skill Score (FSS): The Fractions Skill Score (FSS) [15] is a neighborhood-based metric that evaluates the spatial similarity between forecast and observed precipitation fields. Unlike pixel-wise scores, FSS accounts for small spatial shifts, making it especially suitable for evaluating precipitation forecasts where minor misalignments are common.

First, binary probabilities (BP) are computed using a rainfall threshold range $[q_1, q_2]$:

$$\text{BP}_i = \begin{cases} 1 & \text{if } q_1 \leq F_i < q_2 \\ 0 & \text{otherwise} \end{cases} \quad (4)$$

Where F_i is the rainfall value at grid point i , and q_1, q_2 define the category bounds (in mm/h).

Neighborhood probabilities (NP) for predicted and observed fields are then calculated:

$$\text{NP}_i = \frac{1}{J} \sum_{j=1}^J \text{BP}_{ij} \quad (5)$$

The Fractions Brier Score (FBS) is then calculated as:

$$\text{FBS} = \frac{1}{I} \sum_{i=1}^I (\text{NP}_{i,p} - \text{NP}_{i,o})^2 \quad (6)$$

The Worst Possible FBS (WFBS) is defined as:

$$\text{WFBS} = \frac{1}{I} \sum_{i=1}^I ((\text{NP}_{i,p})^2 + (\text{NP}_{i,o})^2) \quad (7)$$

Finally, the FSS is computed as:

$$\text{FSS} = 1 - \frac{\text{FBS}}{\text{WFBS}} \quad (8)$$

Where I is the number of valid prediction-observation pairs, J the number of neighboring cells. $(\text{NP}_{i,p})$ and $(\text{NP}_{i,o})$ denote predicted and observed neighborhood probabilities, respectively.

The FSS ranges from 0 (no skill) to 1 (perfect skill). Values above 0.5 are typically interpreted as indicative of useful predictive skill. The FSS is particularly sensitive to neighborhood size: larger neighborhoods smooth out differences and often yield higher scores. In this work, a neighborhood size of 3 was selected to account for minor misalignments corresponding to 1 km shifts for a single value in a radar prediction.

D. Models

Two models were developed based on U-Net architecture: a **radar-only model** and a **multimodal model** combining radar and satellite data. Each model was trained for three lead times (5, 15, and 30 minutes), resulting in six trained models.

Radar-only Model: This model uses a U-Net architecture similar to the RainNet model but uses 3D convolutions instead. The 3D convolutions on the radar input have a depth of 1. The input consists of six consecutive radar frames. For a 5-minute lead time, the model is given radar frames from $t-30$ to $t-5$ and predicts the radar frame at t (5 minutes after the last input). For a 15-minute lead time, the model takes $t-40$ to $t-15$ minutes of radar frames, and for a 30-minute lead time, it takes $t-55$ to $t-30$ minutes.

The encoder downsamples via 3D max pooling ($2 \times 2 \times 1$), while the decoder upsamples accordingly. Skip connections link corresponding levels. Each encoder level includes two Conv3D layers with ReLU activations, with the first layer doubling the channel size. In total, the model includes 20 Conv3D layers, four pooling layers, four upsampling layers, and four skip connections. Its output consists of continuous rainfall estimates in mm/h, which are subsequently mapped to precipitation categories for evaluation. Training was performed using the Adam optimizer (learning rate = 1×10^{-4}) with scheduled decay at epochs 10, 30, and 40 over 50 epochs. The model has approximately 31.4 million parameters.

Multimodal Model: The multimodal model has a similar architecture to the radar-only model, but takes a 12-channel input as depth: one radar band and 11 satellite bands per timestamp, and predicts the next radar frame at time t . Satellite data was preprocessed (cropped to same radar area and upsampled with Lanczos interpolation) to match the radar resolution and area (288×288). The resulting input volume spans six timestamps with 12 channels, yielding an input shape of $288 \times 288 \times 12$. The radar-only model takes input of shape $6 \times 288 \times 288 \times 1$ (time \times height \times width \times channels) while the multimodal takes $6 \times 288 \times 288 \times 12$.

The temporal dimension (six frames) is halved in the encoder via pooling ($2 \times 2 \times 2$) and restored in the decoder through upsampling. The model outputs a single radar frame containing numerical precipitation estimates (mm/h). As shown in Fig. 3, the number of parameters increases to approximately 44 million due to the higher input dimensionality.

E. Loss Function

Two loss functions were evaluated: Mean Squared Error (MSE) and log-cosh. Based on experimental results, the log-cosh loss outperformed MSE in overall prediction quality. The log-cosh loss was adopted from the RainNet model. log-cosh loss is less sensitive to outliers and behaves like MSE for small errors but more robust for larger ones. It is defined as:

$$\text{LogCosh}(y, \hat{y}) = \frac{1}{n} \sum_{i=1}^n \log(\cosh(\hat{y}_i - y_i)) \quad (9)$$

with $\cosh(x) = \frac{e^x + e^{-x}}{2}$.

IV. EXPERIMENTS

A. Setup

We trained and evaluated our models using radar and satellite data from North Rhine-Westphalia (NRW), Germany. Data were split as follows: summers of 2018 and 2019 for training, summer 2020 for validation, and summer 2021 for testing. A total of approximately 141,000 images were collected for the specified period, and these were used for training, evaluation, and testing. Training was conducted on NVIDIA A100 GPUs (80 GB), with the radar-only model using 2 GPUs and the multimodal model using 4 GPUs. Each epoch required 1 hour (radar-only) or 3.5 hours (multimodal). We evaluated models using Critical Success Index (CSI), and Fractions Skill Score (FSS).

B. Comparison Across Lead Times

We compared the radar-only and multimodal models for 5, 15, and 30-minute lead times on the 2021 summer test set. Table I summarizes CSI and FSS for heavy and violent rain.

At 5-minute lead time, the multimodal model improves heavy rain CSI by 5% (0.707 vs 0.672) and violent rain CSI by 0.035, showing better detection of intense cells. At 15 minutes, the gain drops to 1% (0.379 vs 0.368), and by 30 minutes, both models perform poorly, with only a marginal difference (0.141 vs 0.140).

TABLE I: Model performance across lead times on 2021 summer test set.

Lead Time	Category	Metric	Radar-only Model	Multimodal Model
5 min	Heavy	CSI	0.672	0.707
		FSS	0.924	0.938
	Violent	CSI	0.417	0.452
		FSS	0.779	0.801
15 min	Heavy	CSI	0.368	0.379
		FSS	0.677	0.689
	Violent	CSI	0.030	0.039
		FSS	0.104	0.129
30 min	Heavy	CSI	0.140	0.141
		FSS	0.330	0.327
	Violent	CSI	0.000	0.003
		FSS	0.001	0.010

As a result, the multimodal models outperformed the radar-only models in the lead times for both CSI and FSS evaluation metrics.

C. Case Study: NRW Flood 2021

To assess real-world performance, we evaluated the models on the flooding event of July 14, 2021, at 12:55. This event resulted in severe damage and loss of life across western Germany, underscoring the importance of accurate and timely rainfall predictions. The chosen radar image for this event contained significant heavy and violent rainfall, making it a valuable test case.

Table II shows the evaluation of both models for all lead times. The multimodal model consistently outperformed the radar-only model across all metrics. Notably, at the 5-minute lead in the violent rain category, CSI jumps from 0.220 with radar-only to 0.384 with the multimodal model. The higher FSS (0.754 vs 0.526) further confirms the multimodal model's superior spatial accuracy in pinpointing high-intensity rain regions.

Fig. 4 offers additional qualitative insight into the NRW flooding event. Even though Table II indicates only a marginal improvement for the multimodal model at the 30-minute lead time, Fig. 4 shows that its prediction is qualitatively much closer to the ground truth than the radar-only model's. The multimodal model effectively captured the shape, intensity, and distribution of heavy rain cells, which are crucial for issuing early warnings in operational settings. These improvements in qualitative accuracy were especially evident in urban areas that experienced flash flooding.

This case study highlights the added value of incorporating satellite imagery into short-term precipitation nowcasting, particularly for extreme weather events. The inclusion of atmospheric parameters from satellite data helped the model anticipate the buildup of convective storms, offering a more comprehensive understanding of evolving weather dynamics.

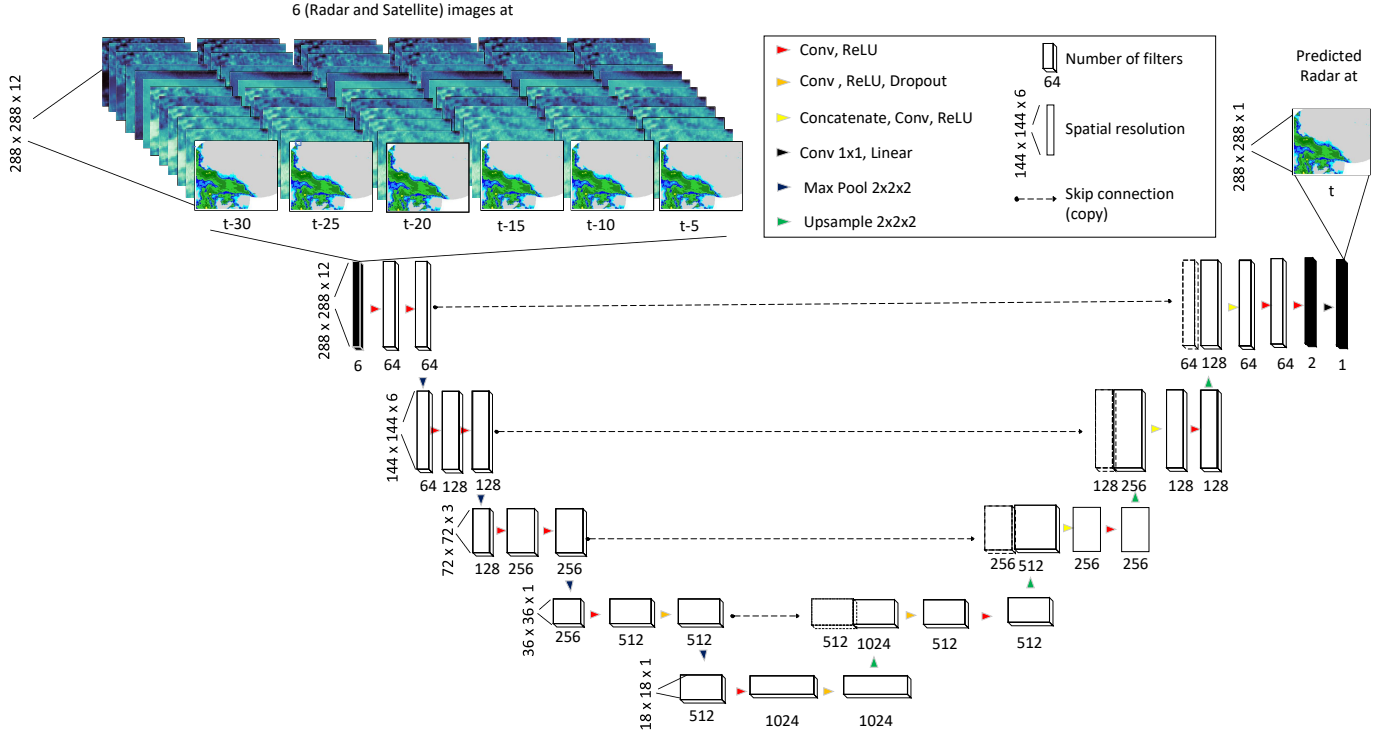


Fig. 3: Architecture of the multimodal model. The model (for 5 min lead time) takes as input a sequence of six time steps (from $t-30$ to $t-5$), where each frame includes 12 channels: 1 radar image and 11 satellite bands. These inputs are processed by a 3D U-Net architecture consisting of 3D convolutional layers, max-pooling, and upsampling operations. The model outputs a single radar image predicting precipitation at t . Skip connections and concatenation operations are used between encoder and decoder stages to preserve spatial and temporal information.

TABLE II: Model performance comparison for NRW flood event (2021-07-14, 12:55) across lead times.

Lead Time	Category	Metric	Radar-only Model	Multimodal Model
5 min	Heavy	CSI	0.801	0.822
		FSS	0.962	0.970
	Violent	CSI	0.220	0.384
		FSS	0.526	0.754
15 min	Heavy	CSI	0.631	0.644
		FSS	0.858	0.869
	Violent	CSI	0.000	0.000
		FSS	0.000	0.000
30 min	Heavy	CSI	0.414	0.419
		FSS	0.662	0.664
	Violent	CSI	0.000	0.000
		FSS	0.000	0.000

V. CONCLUSION

This work introduced a multimodal model combining radar and satellite data to improve short-term precipitation nowcasting at lead times of 5, 15, and 30 minutes. The models were trained on summer data from 2018–19, validated in 2020, and tested in 2021, focusing on convective rainfall.

The results show that the integration of satellite data with radar observations significantly enhances the capacity to detect and predict convective storms, particularly during their formative stages—where radar alone often falls short with longer lead times. Satellite imagery improves the model’s understanding of atmospheric conditions, leading to better forecasts of precipitation spatial distribution and intensity. Qualitative evaluations confirm these improvements, particularly during the July 2021 flood event as shown in Fig. 1 and Fig. 4.

This work focused on comparing predictive performance across different data sources using a fixed architecture. Future research could explore expanding the training dataset to include additional regions and employing more advanced architectures, such as transformers, to further improve nowcasting performance. Additionally, analyzing the individual contribution of satellite bands to prediction accuracy presents a promising direction.

ACKNOWLEDGMENT

This paper, as part of the "heavyRAIN" project (funded by the mFUND program financed by the German Federal Ministry of Transport), explores satellite data collection, data preprocessing, and the development of multimodal models integrating radar and satellite data to enhance nowcasting accuracy and early warning system.

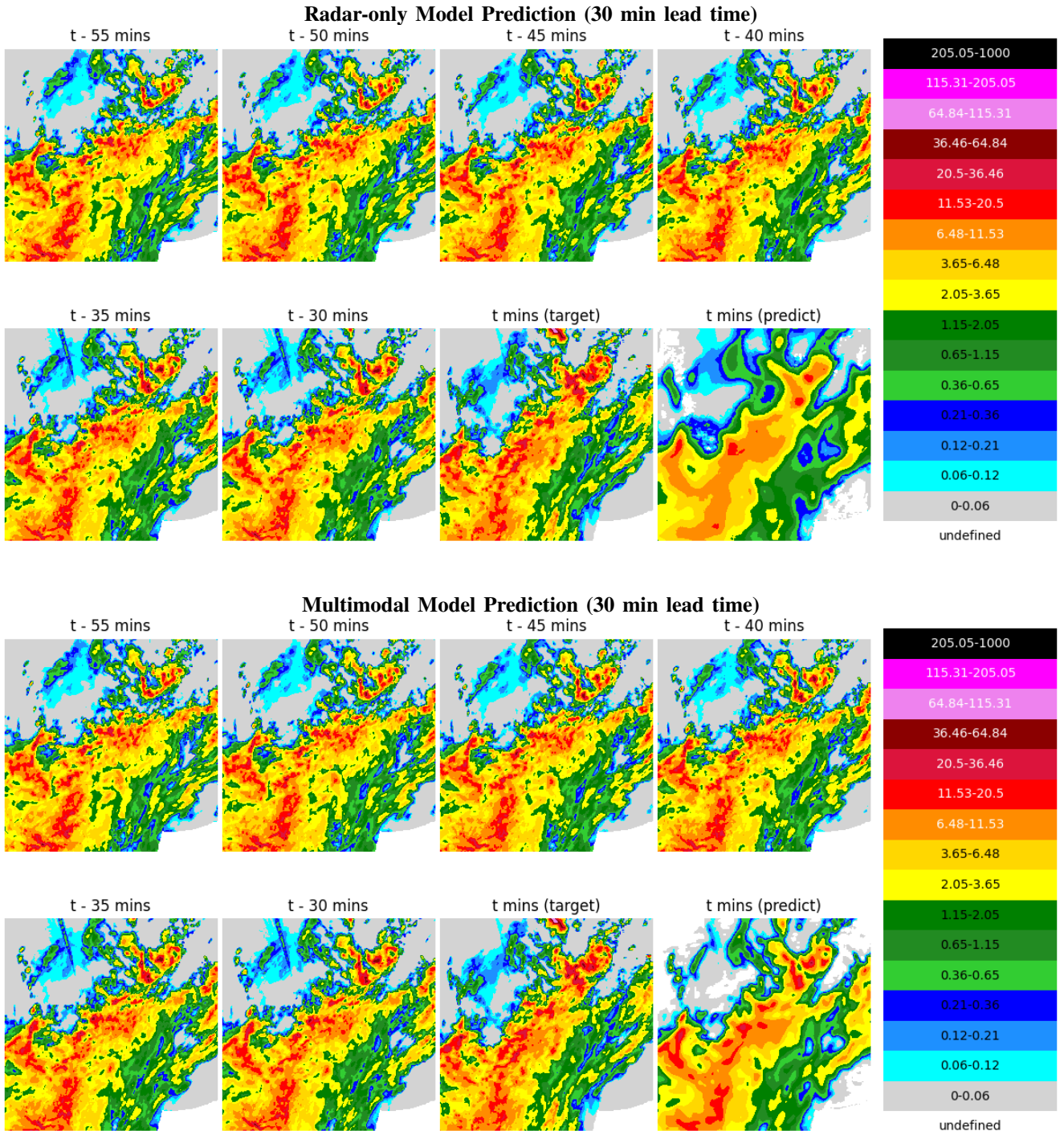


Fig. 4: This figure shows the ground truth radar image (target) of a flooding event in North Rhine-Westphalia on July 14, 2021, along with the predictions at time t from two models: a Radar-only model and a Multimodal model. Both models use the same input sequence of radar images from $t-55$ to $t-30$ minutes. Additionally, the Multimodal model uses satellite images from the same time period. The color bar on the right indicates precipitation intensity in mm/h. The Multimodal model clearly outperforms the Radar-only model, particularly in regions of heavy rainfall, where the Radar-only model underestimates the intensity of the event.

REFERENCES

- [1] M. Kotz, S. Lange, L. Wenz, and A. Levermann, "Constraining the pattern and magnitude of projected extreme precipitation change in a multimodel ensemble," *Journal of Climate*, vol. 37, no. 1, pp. 97–111, 2024.
- [2] Bundeszentrale für politische Bildung (bpb). (2021) Jahrhunderthochwasser 2021 in deutschland. Accessed: 20-Sep-2025. [Online]. Available: <https://www.bpb.de/kurz-knapp/hintergrund-aktuell/337277/jahrhunderthochwasser-2021-in-deutschland/>
- [3] K. Lengfeld, P.-E. Kirstetter, H. J. Fowler, J. Yu, A. Becker, Z. Flamig, and J. Gourley, "Use of radar data for characterizing extreme precipitation at fine scales and short durations," *Environmental Research Letters*, vol. 15, no. 8, p. 085003, 2020.
- [4] F. Cánovas-García, S. García-Galiano, and F. Alonso-Sarría, "Assessment of satellite and radar quantitative precipitation estimates for real time monitoring of meteorological extremes over the southeast of the iberian peninsula," *Remote Sensing*, vol. 10, no. 7, p. 1023, 2018.
- [5] K. Friesenbichler, L. Ialongo, P. Klimek, A. Renhart, and F. Sinabell, "A rapid assessment of the economic impact of the central european flood 2024 on austria," Supply Chain Intelligence Institute Austria (ASCI), Tech. Rep., 2024. [Online]. Available: https://asci.ac.at/wp-content/uploads/ResearchBrief_080924.pdf
- [6] EUMETSAT, *MSG Level 1.5 Image Data Format Description*, EUMETSAT, 2017, https://www-cdn.eumetsat.int/files/2020-04/pdf_ten_msg_seviri_instrument.pdf.
- [7] X. Shi, Z. Chen, H. Wang, D.-Y. Yeung, W.-K. Wong, and W.-c. Woo, "Convolutional lstm network: A machine learning approach for precipitation nowcasting," *Advances in neural information processing systems*, vol. 28, 2015.
- [8] G. Ayzel, T. Scheffer, and M. Heistermann, "Rainnet v1.0: a convolutional neural network for radar-based precipitation nowcasting," *Geoscientific Model Development*, vol. 13, no. 6, pp. 2631–2644, 2020.
- [9] V.-S. Ionescu, G. Czibula, and E. Mihuleț, "Deeps at: A deep learning model for prediction of satellite images for nowcasting purposes," *Procedia Computer Science*, vol. 192, pp. 622–631, 2021.
- [10] J. Pihrt, R. Raevskiy, P. Šimánek, and M. Choma, "Weatherfusionnet: Predicting precipitation from satellite data," *arXiv preprint arXiv:2211.16824*, 2022.
- [11] Y.-J. Park, D. Kim, M. Seo, H.-G. Jeon, and Y. Choi, "Data-driven precipitation nowcasting using satellite imagery," in *Proceedings of the AAAI Conference on Artificial Intelligence*, vol. 39, no. 27, 2025, pp. 28 284–28 292.
- [12] German Meteorological Service (DWD). (2024) Weather radar composites. [Online]. Available: <https://opendata.dwd.de/weather/radar/composite>
- [13] Barani Design, "Rain rate intensity classification," 2020, [Online; accessed 20-August-2024]. [Online]. Available: <https://www.baranidesign.com/faq-articles/2020/1/19/rain-rate-intensity-classification>
- [14] EUMETSAT. (2024) SEVIRI Level 1.5 Rapid Scan Product). [Online]. Available: <https://navigator.eumetsat.int/product/EO:EUM:DAT:MSG:MSG15-RSS>
- [15] L. Wolfgruber, T. Necker, L. Kugler, M. Weissmann, M. Dorninger, and S. Serafin, "The fractions skill score for ensemble forecast verification," Copernicus Meetings, Tech. Rep., 2024.